

GEOLOGY OF THE CYPRUS PIMA MINE, PIMA COUNTY, ARIZONA

by

Joseph D. Langlois¹Abstract

The Cyprus Pima copper deposit, Pima County, Arizona, has recorded a production of over 146 million tons of ore since discovery in 1950. Orebody host rocks include altered Mesozoic arkose and siltstone and Paleozoic silty to sandy limestone altered to hornfels and tactite. The sedimentary section has been intruded by an early Tertiary quartz monzonite porphyry. Subsequent to the intrusion and formation of the orebody, the mine vicinity was intruded by thin, mid-Tertiary andesite dikes. The area was then buried by late Tertiary to Quaternary conglomerate and alluvium.

Intense preore and postore structural deformation has affected the deposit. Preore fracturing is demonstrated by the stockwork pattern of mineral distribution in the host rocks. Postore deformation is also present along both high- and low-angle faults. Some low-angle faults in the mine vicinity truncate ore horizons, and other low-angle structures may have as much as 10 km of displacement.

The orebody is dominantly a primary chalcopyrite deposit with by-product molybdenite. The bulk of ore tonnage is produced from the Mesozoic clastic section, and the higher grade sections in the deposit tend to be located in tactite zones. Major controls for the distribution of the orebody are structural and lithologic.

Introduction

The Cyprus Pima mine is located in the Pima mining district (Fig. 1) approximately 20 miles south of the city of Tucson in Pima County, Arizona. Situated on the eastern pediment surface of the Sierrita Mountains, the Cyprus Pima mine is a significant producer in one of the largest porphyry copper districts in the United States, with a districtwide rated production of about 200,000 tons of ore per day (Heinrichs, 1976).

Previous Production and History

The Pima mining district has had a long and varied history of activity extending back to Spanish colonial times. In 1872 the first mining claim in the Arizona territory, the San Xavier, was located in the Pima mining district to the west of the present Cyprus Pima mine. Early production in the district was supplied by small producers shipping ores containing silver, copper, zinc, gold, lead, and molybdenum. These ores were obtained from underground operations mining small

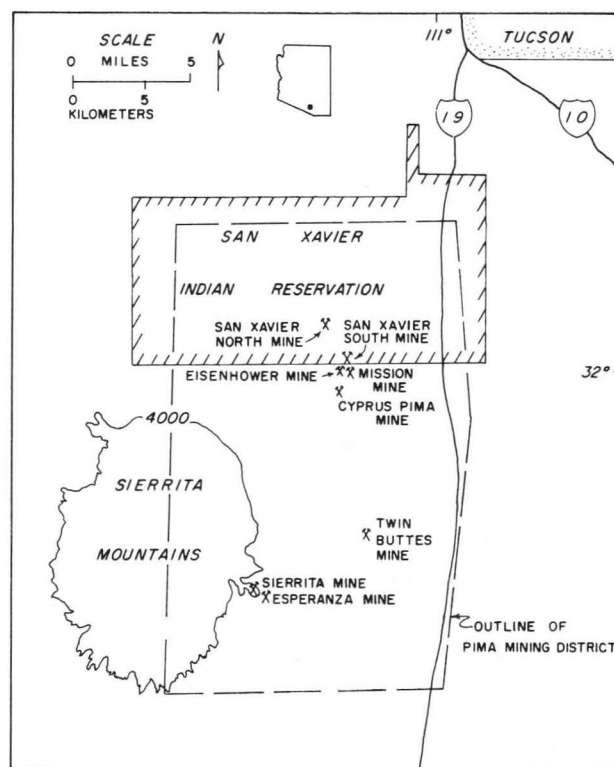


Fig. 1. Location map for Cyprus Pima mine

¹Cyprus Pima Mining Company, Tucson, Arizona 85719

tonnage replacement and contact metamorphic deposits.

Interest in the present Cyprus Pima mine was initiated at the suggestion of Dr. B. S. Butler, a renowned economic geologist at The University of Arizona. Based in part on this suggestion, United Geophysical Company decided to test and evaluate this property where it was believed that geophysical methods might provide useful exploration tools (Heinrichs, 1976). Prospecting permits for the area were obtained in 1950, and an exploration drilling program based on geological and geophysical factors was begun. Shortly thereafter, the first discovery hole was completed and after continued exploration a decision was made to develop a small underground mine.

In 1952 the first shipments of ore were made to smelters, and in that same year United Geophysical Company was acquired by the Union Oil Company. In 1955 the Union Oil Company sold a half interest in the underground mine to Cyprus Mines Corporation and also sold a quarter interest to Utah International Corporation. During the same year a decision was made to convert from underground to open-pit mining operations. Various expansions of the open-pit operation have resulted in a current capacity of 53,500 tons of ore per day. At present over 146 million tons of ore have been produced since the beginning of operations.

Stratigraphy

Lithologic complexity and variety characterize the Cyprus Pima deposit. Altered rocks of sedimentary and igneous origin ranging in age from Paleozoic to Tertiary are related to the orebodies. Recognition of formations, especially within the Paleozoic section, is complicated by indistinct lithologic boundaries, subsequent alteration, and intense faulting. A generalized stratigraphic section for Cyprus Pima mine is present in Figure 2.

The oldest rocks present within the pit vicinity are of Permian age. Although the Permian section is intensely altered and recrystallized and all fossil remains are obliterated, the section consists of some of the dominantly marine carbonate members of the Pennsylvanian-Permian Naco Group of southern Arizona. Based on lithologic characteristics, the altered rocks in the pit vicinity belong to the Colina Limestone, Epitaph Formation, Scherer Formation, and Concha Limestone members of the Naco Group. According to Kinnison and Barter (1976), the minimum aggregate thickness of these units in the Pima district is 1,600 feet. Contacts between and within formations are commonly represented by faults of varying at-

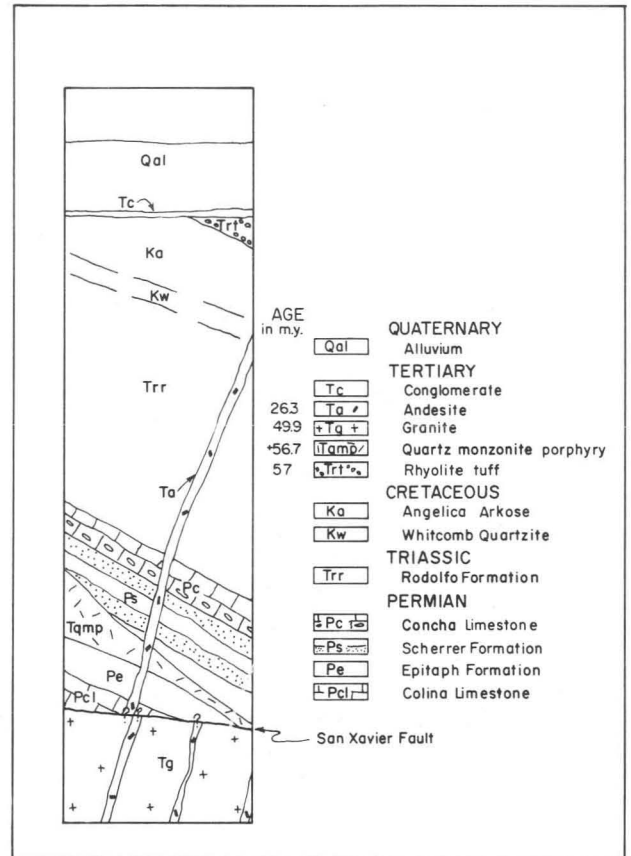


Fig. 2. Generalized stratigraphic section at the Cyprus Pima mine

titude and displacement. Based on geologic mapping at the Mission mine, the Permian sequence is in reverse lithologic order (Jansen, 1976). Mineralization, when present in the altered carbonate lithologies, is best developed in the Concha Limestone and the Epitaph Formation. Thickness of the Permian rocks within the pit vicinity is variable, up to 600 to 700 feet.

Mesozoic rocks within the pit vicinity consist of continental to subaqueous clastic sedimentary rocks of Triassic and Cretaceous age (Cooper, 1971). In the type section for the Triassic Rodolfo Formation, the lithologies include red beds, siltstone, and volcanic members with a thickness in excess of 2,400 feet. In the mine vicinity approximately 1,000 feet of possible Rodolfo Formation is present. This formation, as subdivided in the pit by Himes (1973), consists of argillite, arkose, and lithic arenite. The unit is generally massively bedded and probably correlates with the middle siltstone member of the Rodolfo Formation of Cooper (1971). Contacts of the Rodolfo Formation with overlying Cretaceous rocks are diffuse and gradational. However, the lower contact between Permian carbonate rocks and

the Rodolfo Formation appears in part to be a low-angle fault of unknown displacement developed along an unconformity.

Cretaceous units within the mine vicinity may include both the Whitcomb Quartzite and the Angelica Arkose of Cooper (1971). In the type area the Whitcomb Quartzite consists of 300–600 feet of quartz arenite and rhyolitic tuff. Such a lithologic sequence is not at present recognized within the pit vicinity.

The Angelica Arkose in the type locality comprises over 5,500 feet of volcanoclastic, siltstone, sandstone, arkose, and conglomerate lithologies (Cooper, 1971). In the mine vicinity interbedded sections of arkose, subarkose, lithic arenite, and siltstone exposed along upper benches of the south and east walls of the pit are correlated with the Angelica Arkose with the thickness of these units up to 400 feet. Contacts of the Angelica Arkose with lower units are gradational and diffuse.

In terms of importance to mineralization, the Mesozoic rocks are volumetrically the major host and in particular the Rodolfo Formation currently supplies the bulk of the ore tonnage mined. With an 0.03% Cu cutoff grade, 75 percent of the total volume of ore-grade material mined is produced from Mesozoic rocks.

Tertiary rocks in the mine vicinity include a rhyolite tuff, quartz monzonite porphyry, granite, and an andesite. K-Ar age data for some of these rocks are reported in Table 1 (Shafiqullah, 1976). The rhyolitic tuff, also referred to as biotite rhyolite, is mapped by Cooper (1973) just beyond the southeastern fringe of the pit limit. The contact with underlying Angelica Arkose is gradational and may in part be intermixed with arkosic to volcanoclastic sections of the Angelica Arkose. As recognized in drill core to the southeast of the pit limit, the tuff consists of shards and xenocrysts in a variable matrix at least in part of volcanoclastic origin. Sulfide mineralization in the form of pyrite is present as disseminations and veinlets in the tuff. A K-Ar analysis on biotite from a tuff sample located about one mile south of the mine yielded a date of 57 m.y. (Creasey and Kistler, 1962).

The quartz monzonite porphyry exposed within the pit is an altered, sill-like mass that thickens to the northwest. Phenocrysts of biotite, plagioclase, quartz, and rare K-feldspar are set in a xenomorphic matrix of quartz and feldspar. Most contacts of the porphyry are faulted and the present sill-like configuration of the porphyry may be controlled by low-angle faults at upper and lower con-

tacts. Beneath the southwestern section of the pit the porphyry is separated from a younger granite by a low-angle fault zone correlated with the San Xavier fault. Sulfide mineralization in terms of veinlets and disseminations dominated by pyrite is scattered throughout the porphyry. An age date of 56.7 m.y. was obtained from sericite in crosscutting quartz-sericite-pyrite veins in the porphyry (Table 1) (Shafiqullah, 1976).

The porphyry intrusion at the Cyprus Pima mine may be related to late-stage differentiates of the Laramide Ruby Star granodiorite batholith exposed to the south and west of the mine in the core of the Sierrita Mountains. The 58–60 m.y. age of the batholith, as reported by Creasey and Kistler (1962) and Damon and Mauger (1966), is close to the age of alteration of the porphyry from this report. In addition, the similar age of the rhyolite tuff to the granodiorite may indicate a genetic relation to the Ruby Star batholith.

Below the Cyprus Pima pit is a granite of Tertiary age separated from upper-plate lithologies of Paleozoic, Mesozoic, and Tertiary rocks by a low-angle fault correlated with the San Xavier structure of Cooper (1960). This granite is a medium- to coarse-grained, microcline granite that is weakly propylitized. Mineralization in this granite is extremely sparse with scattered grains of pyrite, chalcopyrite, and molybdenite with metal values averaging less than a hundred parts per million. A K-Ar age date on a biotite concentrate from the granite yielded a date of 49.9 m.y. (Shafiqullah, 1976).

Diamond drilling along the northeast corner of the pit has encountered a series of biotite andesite dikes. A generalized log for one drill-hole intersection of these dikes is shown in Figure 3. The andesite dike is postmineralization in age, and from Figure 3 it may be seen that the dike is cut by a fault zone correlated with the San Xavier fault. Because of the age relationship between the fault and the dike, a biotite separate was obtained from the andesite and a K-Ar date of 26.3 m.y. was obtained (Shafiqullah, 1976). However, the amount of displacement of the dike along the fault was indeterminate.

Covering the Cyprus Pima deposit to a thickness of as much as 250 feet is a sequence of gravels of possible Pliocene-Pleistocene age (Kelly, 1976). A calcite-cemented conglomerate up to 40 feet thick is commonly found above the bedrock surface and at the base of the unconsolidated gravels. The alluvium and conglomerate were deposited on an oxidized bedrock surface.

Table 1. K-Ar ages of rocks from the Cyprus Pima mine

Sample No.	Description and Location	Material Dated	Radiogenic $^{40}\text{Ar} \times 10^{-10}$		Percent Atmospheric ^{40}Ar	Calculated Age in m.y. ¹
			K%	mole/gm		
UAKA-74-89	Porphyritic biotite andesite from drill core hole A414 at Cyprus Pima mine; lat $31^{\circ}59'$, long $111^{\circ}04'$, Twin Buttes quad., Pima Co., Ariz.	biotite, slightly chloritized	6.91	316.1 319.6	7.91 7.16	26.3 ± 0.6
UAKA-75-116	Biotite granite from drill core hole A180 at Cyprus Pima mine. Sample taken 500' below San Xavier fault surface; lat $31^{\circ}59'$, long $111^{\circ}04'$ Twin Buttes quad., Pima Co., Ariz.	biotite, slightly chloritized	7.37	653.4 640.2	8.2 8.2	49.9 ± 1.0
UAKA-75-118	Composite sample of coarse sericite muscovite alteration envelopes cutting quartz monzonite porphyry at Cyprus Pima mine on 2710 bench; lat $31^{\circ}59'$, long $111^{\circ}04'$, Twin Buttes quad., Pima Co., Ariz.	sericite-muscovite	8.41	847.7 833.9	4.8 5.2	56.7 ± 1.2

¹ Constants: $\lambda_e = 0.575 \times 10^{-10} \text{ yr}^{-1}$, $\lambda_\beta = 4.905 \times 10^{-10} \text{ yr}^{-1}$, $^{40}\text{K}/\text{K} = 1.18 \times 10^{-4} \text{ g}^{40}\text{K}/\text{gK}$

Structure

Structural development of the Pima mining district in general and the Cyprus Pima deposit has been complex and varied. The structural complexity of a portion of the district from the Twin Buttes mine to the Cyprus Pima mine is illustrated in Figure 4.

Lacy (1959) recognized various periods of structural development in the district. The older premineralization structural features included folding, steep left-lateral faulting, normal faulting, and low-angle "thrust" faulting. Drewes (1976) also recognized on a regional basis in southern Arizona early premineralization thrust faults and indicated that the thrust development was most active about 75-80 m.y. ago.

Lacy also recognized another period of postmineralization "thrusting" involving the Oligocene Helmet Fanglomerate and andesite dikes. This later period of low-angle faulting is correlative with the San Xavier fault of Cooper (1960). In the Pima mining district,

Cooper has proposed that the San Xavier "thrust" fault (or gravity glide fault, Drewes, 1976) was of postmineralization age but pre-andesite dike swarm age (24-26 m.y.) and that the fault had a displacement of about 10 km in a north-northwest direction. Cooper (1971) also suggested that the Cyprus Pima-Mission mines are the displaced upper portions of the Twin Buttes copper deposit located about 10 km to the south.

A generalized geological section from the Twin Buttes area to the Cyprus Pima mine area is presented in Figure 5, adapted from Cooper (1973), Kelly (1976), Weaver (1971), and diamond-drill information. The age of 56.7 m.y. for the sericitic alteration establishes a Laramide age for mineralization and is very close to an age of 57.1 m.y. obtained from the quartz monzonite porphyry at the Twin Buttes deposit (Kelly, 1976). A 49.9-m.y. age for the granite beneath the San Xavier fault requires an age of fault development younger than the granite and the mineralization. Cooper (1960) also concluded that the age of movement along the fault was younger

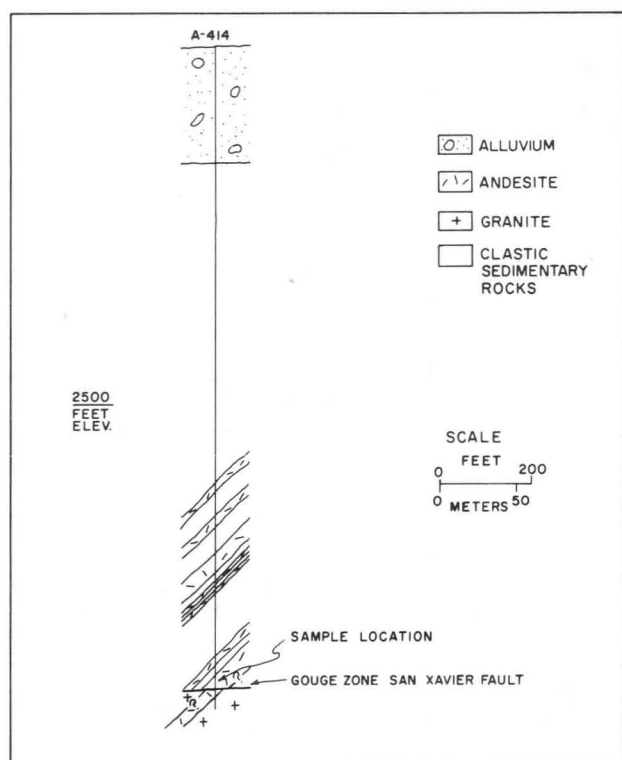


Fig. 3. Generalized log of diamond drill hole showing San Xavier fault cutting andesite dikes

than the Oligocene Helmet Fanglomerate. Because the San Xavier fault cuts a 26.3-m.y. andesite dike in the mine area, at least some of the movement along the fault is younger than the andesite dike event. Therefore, the age of movement along the San Xavier structure is interpreted to be postmineralization and probably extended through late Oligocene to early Miocene time.

Within the pit vicinity the attitude of the Paleozoic and Mesozoic sedimentary rocks varies from N. 60°-75° E. with dips ranging from 45°-65° SW. (Dames and Moore, 1976). Detailed structural data related to orientation of faulting and jointing were collected by Himes (1973) and Dames and Moore (1976). Two major directions of faulting were found: N. 50°-60° E. and N. 40°-50° W. These data are compatible with the principal Laramide trends as reported by Rehrig and Heidrick (1972). Dames and Moore (1976) also noted an additional major fault attitude of N. 10°-20° W. According to Rehrig and Heidrick (1976) this direction corresponds to late Tertiary structural trends.

Measured joint patterns are much more variable. The east-northeast and the northwest strike directions for joints again are compatible with Laramide trends. Attitudes of N. 0°-

20° W. for joints correspond to late Tertiary structural directions. Other joint orientations, such as N. 12° E. as reported by Himes (1973), are of uncertain age and origin.

Figure 6 presents a generalized geologic map at the 2670 elevation, and Figure 7 shows a generalized contour map of the San Xavier fault surface in the mine vicinity. From the contour map the gentle eastward-dipping slope of the fault surface is interrupted by a north-northwest depression in the contours. This depression may be a result of a graben structure or a large mullion structure (Jansen, 1976) related to the San Xavier fault. Figure 7 also shows the location of sections through the Cyprus Pima mine.

Figure 8 shows a northwest-southeast section oriented oblique to the depression in the San Xavier fault surface. From the section high-angle and low-angle structures of various ages may be noted. The generalized sill-like nature of the porphyry intrusion may also be noted. On this section the San Xavier fault, which separates Tertiary granite from altered Paleozoic carbonate rocks, is the youngest structure.

Figure 9 is a northeast-southwest section oriented across the contour depression of the San Xavier fault surface. As in the previous section early high-angle structures are displaced by the San Xavier fault. Other high-angle structures younger than the San Xavier fault have displaced the surface of the fault by hundreds of feet. The eastern edge of the contour depression of the San Xavier fault may be caused by a series of steep en echelon faults as shown on the section, although the possibility of a mullion structure cannot be eliminated.

Alteration

Alteration patterns of the igneous and clastic sedimentary rocks at Cyprus Pima mine are similar to the general mineral assemblages and distributions as reported by Lowell and Guilbert (1970) for other porphyry copper deposits. However, alteration of the Paleozoic marine carbonate sequence by presumably similar pressure-temperature solution composition variables has produced assemblages consisting of garnet, diopside, tremolite, and other Ca-Mg silicates.

The Mesozoic clastic section and the quartz monzonite porphyry show abundant evidence of potassic and, to a lesser extent, sericitic alteration (Himes, 1973). Secondary K-feldspar as alteration halos and as massive wall-rock replacement is common in the clastic

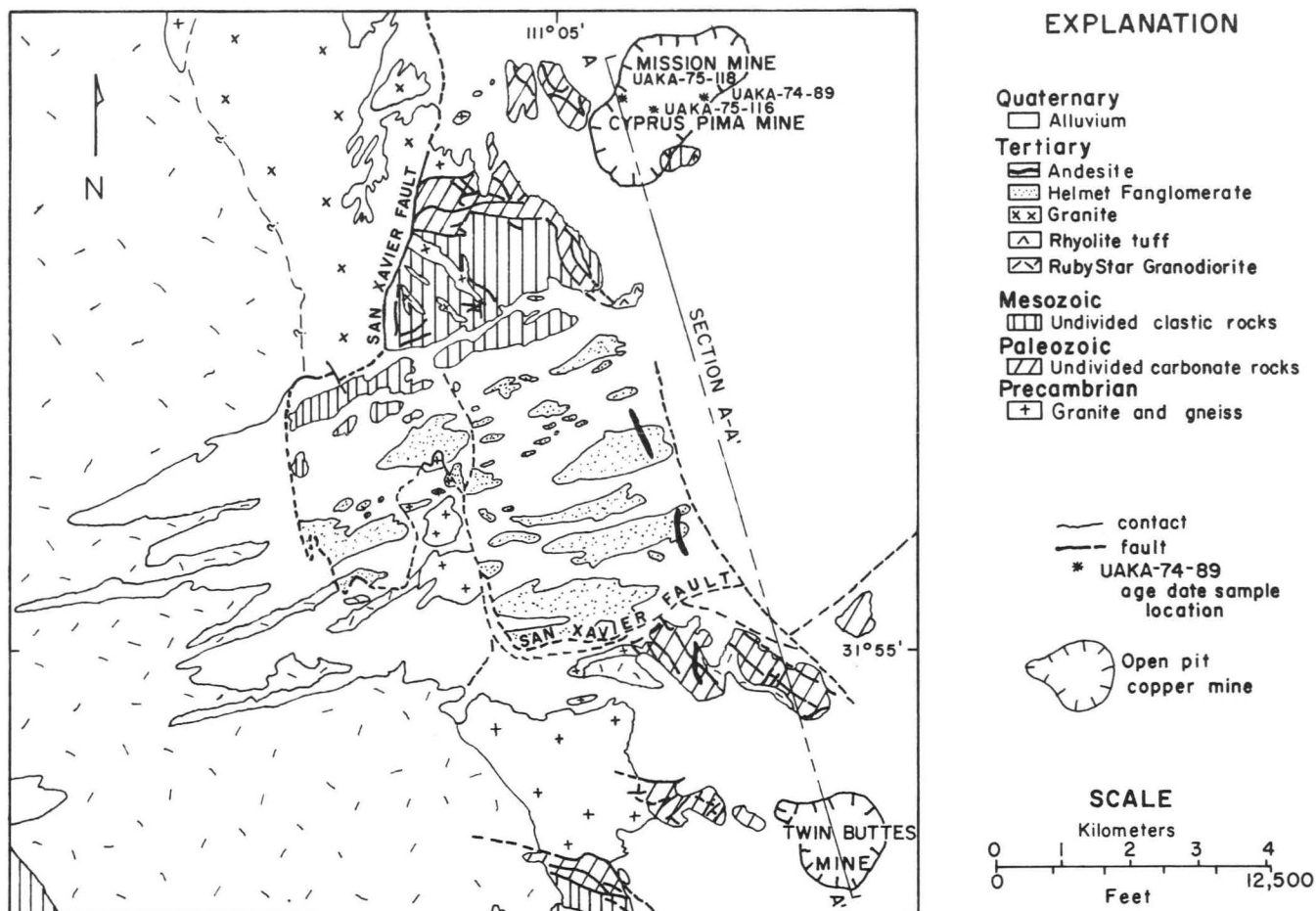


Fig. 4. Generalized geologic map of a portion of the Pima mining district extending from the Cyprus Pima mine to the Twin Buttes mine—adapted from Cooper (1973)

sedimentary rocks and the quartz monzonite porphyry. Common associates of this assemblage are sericite, calcite, anhydrite, and sulfides.

Sericitic or phyllic alteration is generally restricted to vein alteration halos ranging from 1 to 5 cm wide. The alteration assemblage is characterized by feldspar-destructive quartz, sericite-muscovite, and sulfides with the sericitic veins and alteration halos crosscutting the potassic alteration mineral assemblages in the quartz monzonite porphyry. Development of the sericitic alteration is best in the quartz monzonite porphyry along the western face of the pit wall. A more diffuse and less distinct zone of sericitic alteration may be present on the upper benches of the east pit wall in the Mesozoic clastic sedimentary rocks.

Propylitic alteration assemblages as recognized by Himes (1973) are generally restricted to the southwestern part of the pit. An assemblage of epidote, chlorite, calcite, quartz,

and sericite is present in Mesozoic clastic rocks together with scattered quantities of sulfides.

Alteration of the Permian carbonate section has produced various types of calcium silicate hornfels and tactites. Pyrometasomatism and recrystallization combined with hydrothermal alteration have resulted in hornfels composed of andradite or grossularite garnet, diopside, tremolite, magnetite, calcite, quartz, and biotite. The distribution of the different types of hornfels is variable and probably reflects initial differences in composition of different facies of impure carbonate lithologies. Sulfides are distributed in the hornfels as local massive clots and in and adjacent to veins.

Crosscutting the tactite sections are veins with associated alteration halos of actinolite, epidote, magnetite, and serpentine. This later stage alteration event may be related to the crosscutting sericitic alteration that developed in the igneous and clastic rocks.

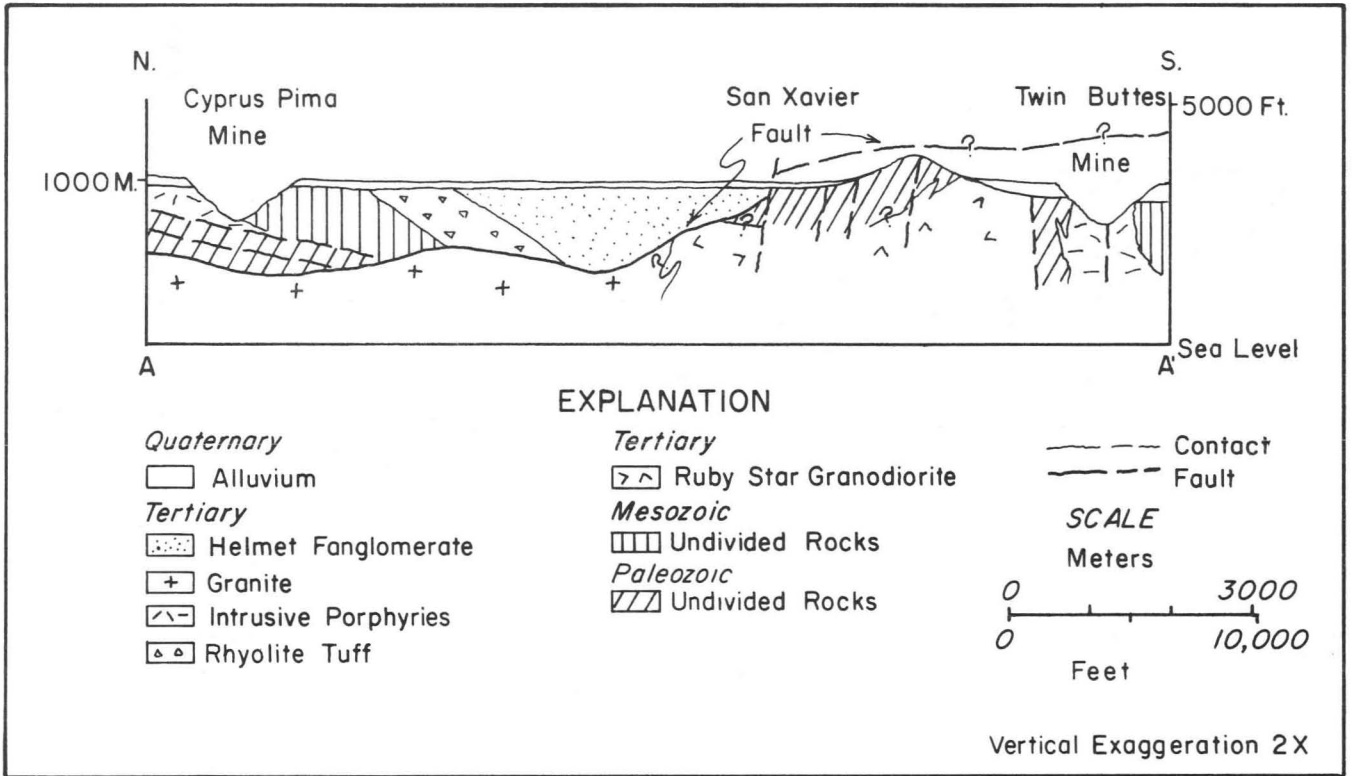


Fig. 5. Geologic section from Cyprus Pima mine to the Twin Buttes mine

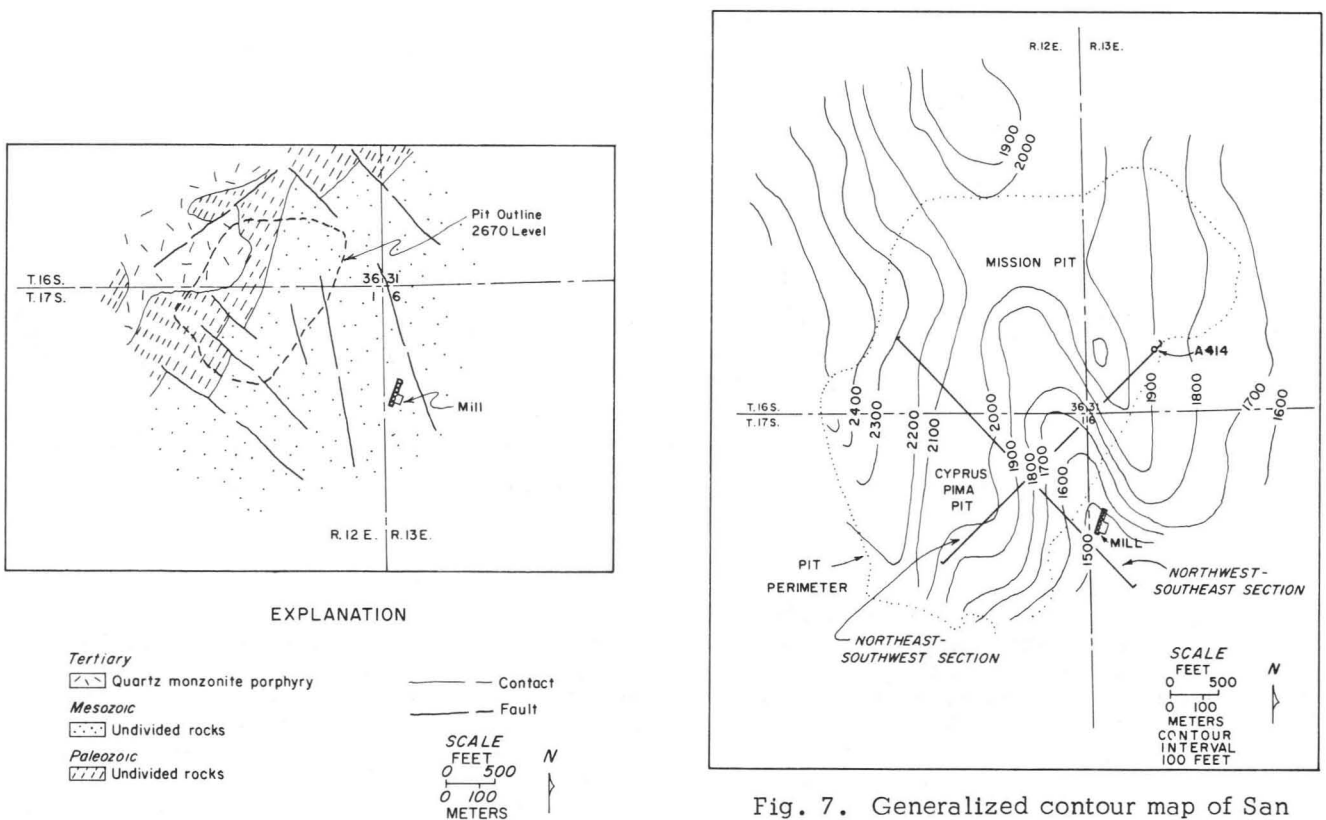


Fig. 6. Geologic map at the 2670 elevation

Fig. 7. Generalized contour map of San Xavier fault surface based on data from the Cyprus Pima and Mission mines

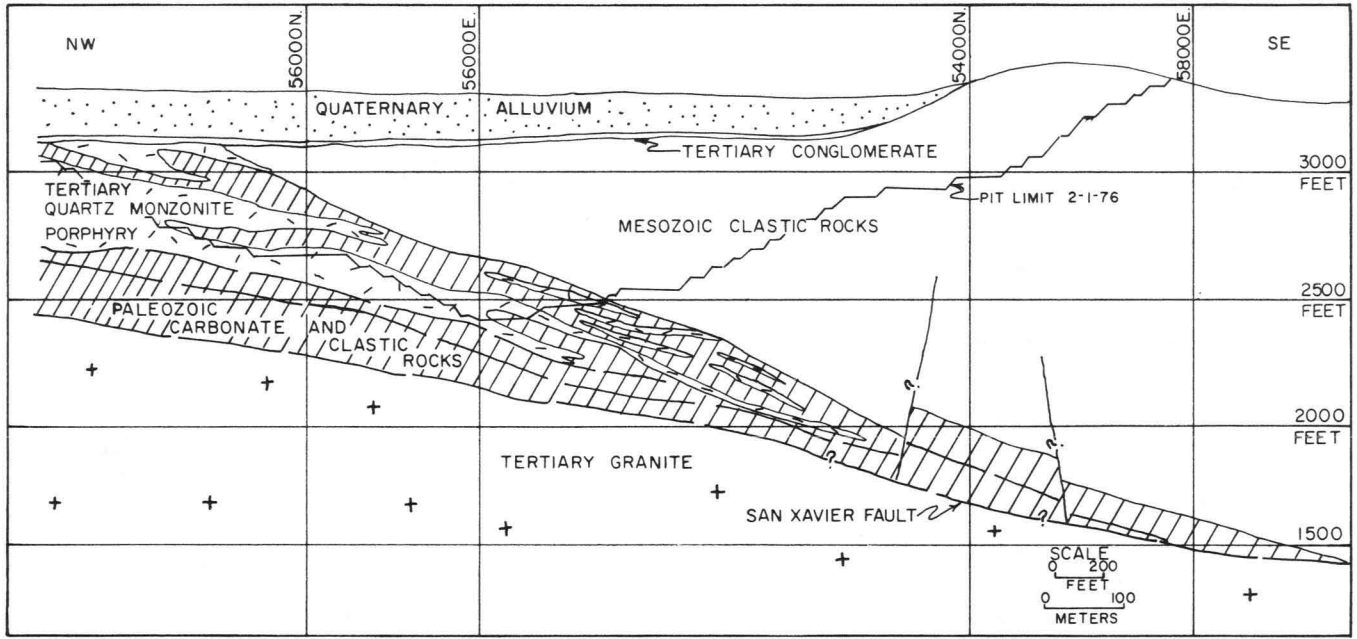


Fig. 8. Northwest-southeast cross section through the Cyprus Pima mine

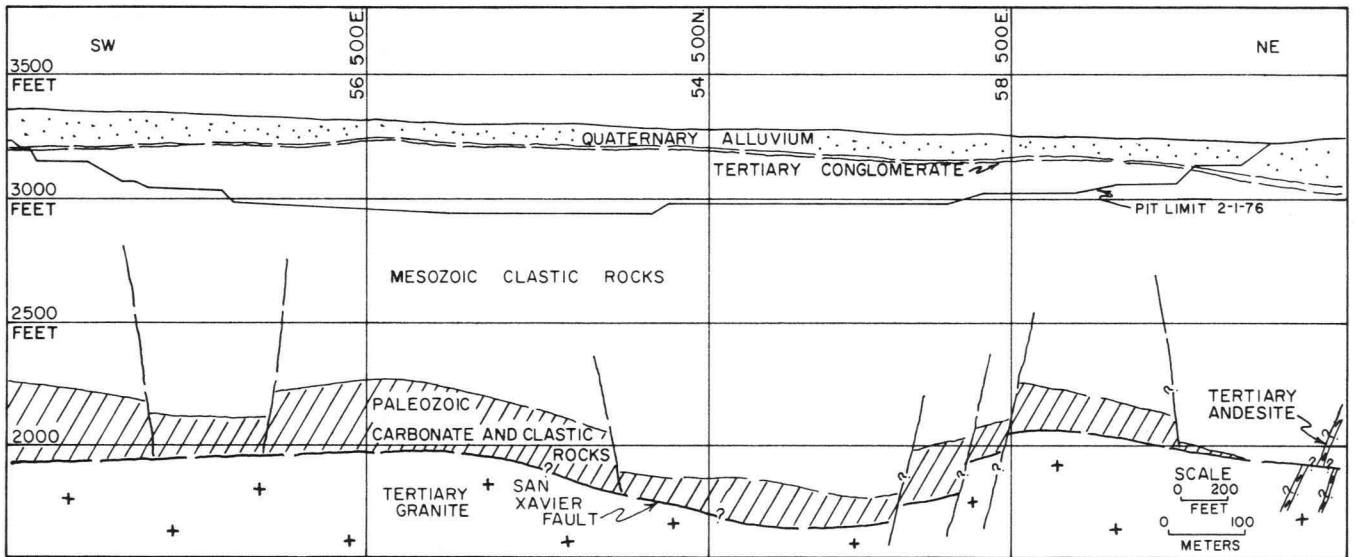


Fig. 9. Northeast-southwest cross section through the Cyprus Pima mine

Supergene alteration effects are largely limited to the development of clay minerals, iron oxides, copper oxides, and sparse chalcocite along upper benches of the pit. Gypsum and calcite are also present as fracture fillings deep within the pit. Alunite of uncertain origin and mixed with clay minerals occurs as fracture fillings along the highest benches of the southeast margin of the pit.

Mineralization

Sulfide mineralization in the Cyprus Pima orebody consists of veinlet, disseminated, and locally massive types with chalcopyrite the dominant copper sulfide. Veinlet and disseminated types in approximately equal proportions are most abundant in the altered Mesozoic clastic sections and massive replacement type sulfide mineralization is largely limited to the altered Paleozoic carbonate lithologies.

Other common sulfide minerals include pyrite and molybdenite with lesser amounts of sphalerite, galena, tennantite-tetrahedrite, chalcocite, bornite, and valleriite. Local massive occurrences of sphalerite, magnetite, and chalcopyrite are limited to tactite bodies present in the western part of the mine. Chalcocite is present only in limited quantities and in small tonnages relative to total reserves near the relatively shallow base of oxidation. According to Parkinson (1976), current average ore grades are 0.47% Cu and 0.015% Mo. Silver is also recovered as a by-product from the ores during the smelting process.

Structural and lithologic controls are important to ore distribution at Cyprus Pima mine. Preore brecciation and stockwork fracturing were the major ore controls. Wall-rock environment as controlled by lithologies also played a major role in sulfide distribution. Table 2 summarizes grade distribution data for each lithologic type based on grade distributions for bench level averages. Assuming that each of the lithologies was subjected to the same structural environment and channelways, the relative order for each lithology as a copper sulfide host based on the statistics is

Table 2. Copper-grade distribution data for bench-level averages from diamond drill holes for various lithologic types

Lithology	Median Grade ¹	Arithmetic Average of Grades	Total Number of Data Points
Paleozoic tactite and hornfels	0.62	0.81	360
Mesozoic clastic rocks	0.33	0.38	1459
Paleozoic quartzite and clastics	0.20	0.23	131
Tertiary quartz monzonite porphyry	0.12	0.15	177
Paleozoic marble and limestone	0.03	0.11	94

¹ 50% cumulative frequency

Paleozoic hornfels, Mesozoic clastic rocks, Paleozoic quartzite, Tertiary porphyry, and Paleozoic limestone.

Figures 10 and 11 show grade distributions based on a 40-foot running average contouring system for the Cyprus Pima deposit. Postmineralization displacement of orebodies is illustrated by these sections. Low-angle structures complementary to the San Xavier fault truncate hornfels ore sections below the porphyry body and hundreds of feet above the San Xavier fault in the northern portions of both sections. The sections also illustrate the relative potential of the Mesozoic clastic section, Paleozoic hornfels, and Tertiary porphyry as orebody hosts.

Molybdenite mineralization, although processed in the milling operation, shows a poor correlation with copper content. Figure 12 graphically illustrates the lack of correlation and a statistically derived correlation coefficient of 0.378 confirms this observation. Inspection of molybdenite occurrences in the mine suggests that molybdenite distribution increases in silica-rich rocks, such as the porphyry and certain clastic units.

Zoning relationships at the Cyprus Pima mine are poorly known. With increasing distance to the east away from the present location of the porphyry, the proportions of tetrahedrite-tennantite and sphalerite to chalcopyrite increase. Bornite occurrence relative to chalcopyrite is highest in slightly marbleized sections below the main ore zone.

Oxide minerals at the Cyprus Pima mine include chrysocolla, tenorite, malachite, and azurite. Because of the relatively small quantities of oxide copper minerals present, oxide ores are not processed.

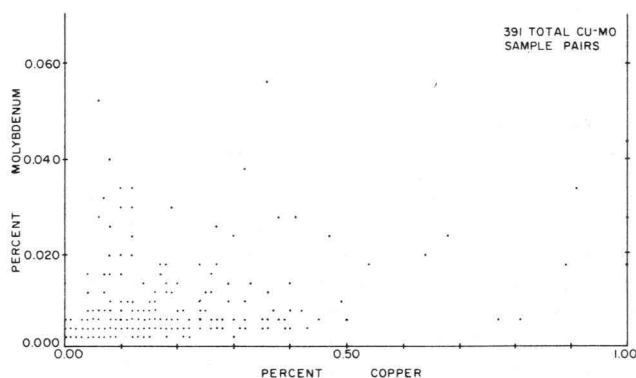


Fig. 12. Plot of corresponding copper and molybdenum bench averages from drill-hole data

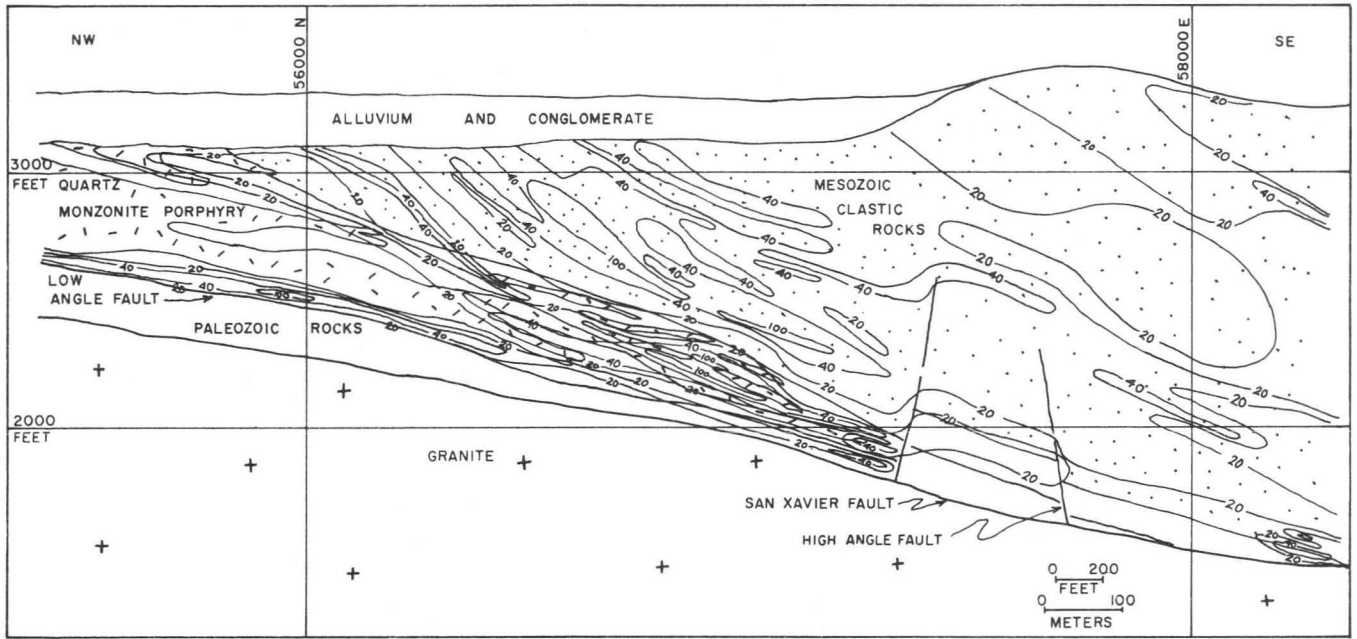


Fig. 10. Grade contour section based on 40-foot running averages for a northwest-southeast section through the Cyprus Pima mine

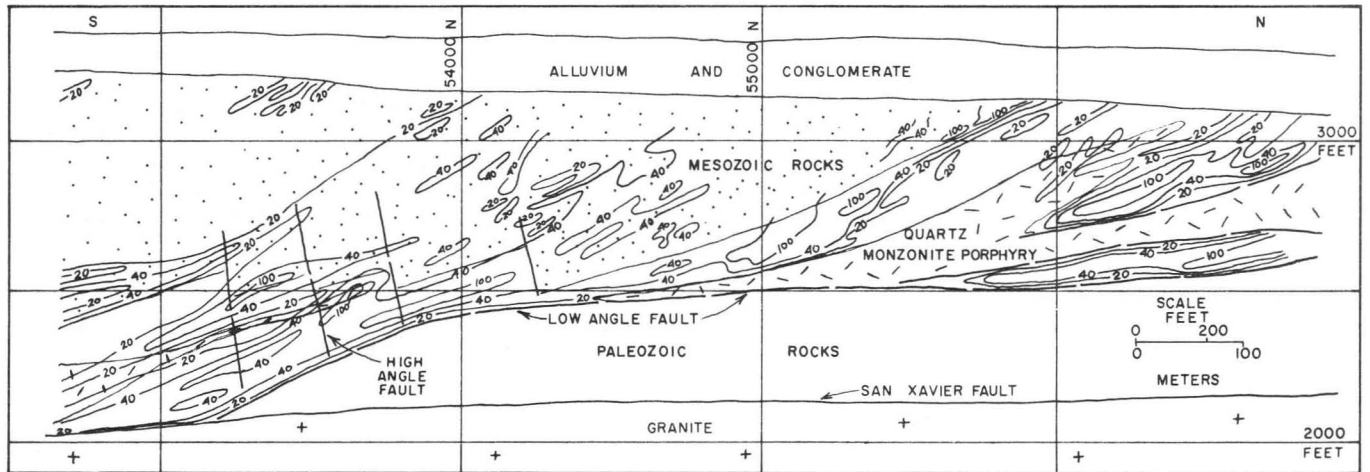


Fig. 11. Grade contour section based on 40-foot running averages for a north-south section through the Cyprus Pima mine

Himes (1973) regards the alteration-mineralization processes at the Cyprus Pima mine as contemporaneous with and related to the emplacement of the quartz monzonite porphyry. Although sulfides appear to preferentially replace calc-magnesian silicates in tactite zones, the alteration-mineralization events probably developed over a continuum of pressure-temperature conditions. Early high-temperature conditions resulted in development of tactite, some K-silicate alteration, and some sulfides. Lower temperature conditions resulted in actinolite, magnetite, and sericitic alteration developed in conjunction with dom-

inantly pyritic sulfides. The present distribution of sulfide ore horizons was a function of premineralization fracturing and favorable lithologic environments and of postmineralization displacement along low-angle fault planes.

Acknowledgments

The author wishes to express his appreciation for critical review and advice concerning the manuscript to Dr. R. Williamson, Chief Geologist at Cyprus Pima Mine.

Appreciation is also extended to the management of Cyprus Pima Mining Company for their permission to prepare this paper. Special thanks are due to Dr. M. Shafiqullah of The University of Arizona for permission to release certain K-Ar age dates and to P. Jobs for typing assistance.

Finally, the author wishes to thank M. Himes and J. Furlow who reviewed the manuscript and expressed their opinions, but the author nevertheless remains solely responsible for any errors of fact or interpretation.

References

- Cooper, J. R., 1960, Some geologic features of the Pima mining district, Pima County, Arizona: U.S. Geol. Survey Bull. 1112-C, p. 63-103.
- _____, 1971, Mesozoic stratigraphy of the Sierrita Mountains, Pima County, Arizona: U.S. Geol. Survey Prof. Paper 658-D, p. 42.
- _____, 1973, Geologic map of the Twin Buttes quadrangle, southwest of Tucson, Pima County, Arizona: U.S. Geol. Survey Misc. Geol. Inv. Map I-745.
- Creasey, S. C., and Kistler, R. W., 1962, Age of some copper-bearing porphyries and other igneous rocks in southeastern Arizona, in Short papers in geology, hydrology, and topography: U.S. Geol. Survey Prof. Paper 450-D, p. D1-D5.
- Dames and Moore, 1976, Slope stability studies, Pima open pit mine, Arizona: Internal company report submitted to Cyprus Pima Mining Co., March.
- Damon, P. E., and Mauger, R. L., 1966, Epeirogeny-orogeny viewed from the Basin and Range province: Soc. Mining Engineers Trans., v. 235, no. 1, p. 99-112.
- Drewes, H., 1976, Laramide tectonics from Paradise to Hells Gate, southeastern Arizona: Arizona Geol. Soc. Digest, v. 10, p. 151-167.
- Heinrichs, W. E., 1976, Pima district, Arizona—a historical and economic perspective: unpublished preprint, A.I.M.E. Annual Meeting, Las Vegas, Nevada, 21 p.
- Himes, M. D., 1973, Mineralization and alteration at Pima mine—a complex porphyry copper deposit: A.I.M.E., S.M.E. Trans., v. 254, no. 2, p. 166-174.
- Jansen, L. R., 1976, Written communication.
- Kelly, J. L., 1976, Geology of the Twin Buttes copper deposit, Pima County, Arizona: A.I.M.E. Preprint 76-I-3, 23 p.
- Kinnison, J. E., and Barter, C. F., 1976, Geology of the Pima mining district: Arizona Geol. Soc., Field Trip Guide 8.
- Lacy, W. C., 1959, Structure and ore deposits of the east side of the Sierrita Mountains, Arizona, in Heindl, L. A., ed., Southern Arizona Guidebook II: Tucson, Arizona Geol. Soc., p. 185-192.
- Lowell, J. D., and Guilbert, J. M., 1970, Lateral and vertical alteration-mineralization zoning in porphyry ore deposits: Econ. Geology, v. 65, p. 373-408.
- Lukanuski, J. N., Nevin, A. E., and Williams, S. A., 1975, Locomotive-type post-ore fanglomerates as exploration guides for porphyry copper deposits: A.I.M.E. Preprint 75-S-35, 18 p.
- Parkinson, G., 1976, Cyprus develops molybdenum separation float: Eng. Mining Jour., May, p. 97.
- Rehrig, W. A., and Heidrick, T. L., 1972, Regional fracturing in Laramide stocks of Arizona and its relationship to porphyry copper mineralization: Econ. Geology, v. 67, p. 198-213.
- _____, 1976, Regional tectonic stress during the Laramide and late Tertiary intrusive periods, Basin and Range province, Arizona: Arizona Geol. Soc. Digest, v. 10, p. 205-228.
- Shafiqullah, M., 1976, Written communication.
- Weaver, R. R., 1971, Uplift and gravitational adjustment, Ruby Star Ranch area, Pima mining district, Arizona: Arizona Geol. Soc. Digest, v. 9, p. 197-211.